FLOOD SUSCEPTIBILITY MAPPING OF URBAN ZARIA, NIGERIA

Bawa Swafiyudeen[1], Akomolafe Ebenezer Ayobami[1], Adamu Bala[1], Aliyu AbdulAzeez Onotu[1] and Moses Mefe[1]
[1]Department of Geomatics, Faculty of Environmental Design, Ahmadu Bello University, Zaria-Nigeria
Email: bswafiyuden@gmail.com

ABSTRACT: Flood is among the natural hazards that affect people's livelihood across the globe. The world bank group in 2020 revealed that about 38.8 million people are exposed to significant flood risk in Nigeria. Therefore, for the first time, in terms of methodology and study area, this study employed multi-source environmental conditioning factors (viz: slope, LULC, soil-type, elevation, rainfall, distance to road network, distance to drainage, Topographic Wetness Index (TWI)) using the Analytical Hierarchy Process (AHP) approach to preparing flood susceptibility map of urban Zaria. About 61% of the area under study is classified as highly susceptible to flood. 36%, 2%, 1%, and less than 1% fall under the moderate class, very high, very low, and low classes of flood susceptibility respectively. Using Area Under the Curve (AUC) an accuracy measure for the flood susceptibility map indicated a considerable value of 0.86. The method adopted in this study is a simple one, yet it reveals significant information that relevant authorities must take into cognizance to mitigate the loss of lives and property.

KEY WORDS: AHP, Flooding, MCD, Remote Sensing and GIS, Sabon-Gari

1. INTRODUCTION

Due to the rapid population growth globally, climatic change, environmental degradation, and poor land-use related issues, amongst others, the occurrence of natural disasters for example volcanic eruptions, landslides earthquakes, hurricanes, and floods have increased significantly in recent times (Caruso, 2017; Dano et al., 2019). These natural disasters result in severe loss of lives and damage to properties, as well as a social and economic imbalance. Among these natural disasters, flood accounts for about 31% of economic damages (Yalcin & Akyürek, 2004) as well as health-related hazards from waterborne ailments (Tehrany et al., 2019). It is among the most pervasive perils affecting people around the globe - about 19% of the world's population is at risk of substantial flooding (Rentschler & Salhab, 2020). Low-income countries with poor infrastructural systems, not limited to poor drainage and flood protection schemes are at higher risk. For example, numerous devastating flooding events have been reported daily across Africa, Americas, Asia, Europe and the Oceania since 2008 to date (floodlist, 2021).

Therefore, the study of the susceptibility of this phenomenon at micro or macro level is a current trend, most especially for floods and floodplain management strategies (Ahmadlou et al., n.d.; Dano et al., 2019; Hammami et al., 2019; Msabi & Makonyo, 2021; Razavi Termeh et al., 2018; Rentschler & Salhab, 2020; Souissi et al., 2020). However, the knowledge of flood occurrence be it fluvial floods (river floods), pluvial floods (flash floods and surface water) or coastal flood (storm surge) (Flood Water, 2020) in varying catchment and climatic scenarios is extremely vital to aid map out susceptible zones for the avoidance of severe destructions (Tehrany et al., 2019).

As highlighted in the reference herein, the concept of flood susceptibility mapping is not new, the methods and strategies of its realization is what varies amongst authors and literatures. This methods can be grouped into three categories (Cabrera & Lee, 2019); (i) Hydrological models such as Soil and Water Assessment Tool (SWAT) (Dano et al., 2019), Hydrologic Engineering Centres River Analysis System (HEC-RAS) (Veleda et al., 2017), FLO-2D (Huang & Qin, 2014), etc. (ii) Quantitative approaches such as frequency ratio (FR) (Tehrany et al., 2019), weights-of-evidence(WE) (Tehrany et al., 2019), logistic regression (LR) (Tehrany et al., 2019), genetic algorithm (GA)(Hong et al., 2018), differential evolution(Hong et al., 2018) and analytic hierarchy process (AHP) (Saaty, 1980), analytical network process (ANP) (Dano et al., 2019) etc. (iii) Machine learning algorithms such as artificial neural network (ANN), support vector machine(SVM) (Tehrany et al., 2019) and random forest (RF) or decision tree (DT) (Tehrany et al., 2013) etc. More detailed conception about these methods and strategies can be found in (Souissi et al., 2020; Tehrany et al., 2019). Among these methods Analytic Hierarchy Process (AHP) which is a multi-criteria decision making (MCDM) developed by (Saaty, 1980) is the most widely used (Cabrera & Lee, 2019; Souissi et al., 2020). For example, (Das, 2020a; Hammami et al., 2019; Razavi Termeh et al., 2018; Rincón et al., 2018; Souissi et al., 2020; Yalcin & Akyürek, 2004) have all found the method suitable for flood susceptibility mapping.

In modelling flood, some conditioning factors play key role. In a previous studies, Tehrany et al., (2019) for example, considered Altitude, slope, aspect, curvature, stream power index (SPI), topographic wetness index (TWI), distance from rivers, (H) distance from roads, rainfall, soil types, geology, land use land cover (LULC) as flood conditioning factors. Similarly Cabrera and Lee, (2019) considered rainfall, slope, elevation, distance to main channel, drainage and soil type. Also Souissi et al., (2020) considered Drainage density map, distance from the drainage network map, Elevation map, Slope map, Rainfall intensity map, Land use/ Land cover map, Groundwater depth and Lithology map. From the foregoing and other references herein, roughly about not less than 5 factors are considered as contributors to flooding. In similar work in our study area, Andongma et al., (2017) considered only slope, elevation,

distance to drainage and wetness index to model flood susceptibility. These factors alone can't be relied upon for accurate flood susceptibility mapping. For example, LULC, soil type, elevation etc. which are major contributors were left out. In the same effort, Mangaji et al., (2020) considered only LULC as a factor. It is also worth mentioning that these studies considered only regions around the major river (River Kubanni). Also, to the knowledge of the current study, this is the first study on flood susceptibility mapping of this depth. Therefore, for the decision support system, this study uses AHP by considering 8 factors (slope, LULC, soil-type, elevation, rainfall, distance to road network, distance to drainage, Topographic Wetness Index (TWI)) to model flood prone areas in Zaria and Sabon-Gari Local government.

2. STUDY AREA

In this study, urban Zaria (Figure 1), is comprised of two local government areas **(**Sabon-Gari and Zaria). It is located between longitude 7° 35' 0"E to 7° 47' 45"E and latitude 11° 09' 23.16"N to 11° 40' 25"N, with an average height of 640meters above mean sea level (MSL) (Dennis, 1944). The main drainage around Zaria is river Galma, which flows in a meandering course with river Shika, Saye, Yashi and Kubanni serving as tributaries and seasonal in nature (Dennis, 1944). Based on Köppen climate classification (Beck et al., 2018), Sabon-Gari Zaria has a tropical savanna climate (Aw) with warm weather all year-round. The region has 2 seasons i.e. wet and dry, lasting from May to September, and October to March respectively. The month of August experiences peak rainfall. The educational setting of the study area contributes to its fast and dynamic physical, economic and social characteristics (Mangaji et al., 2020).

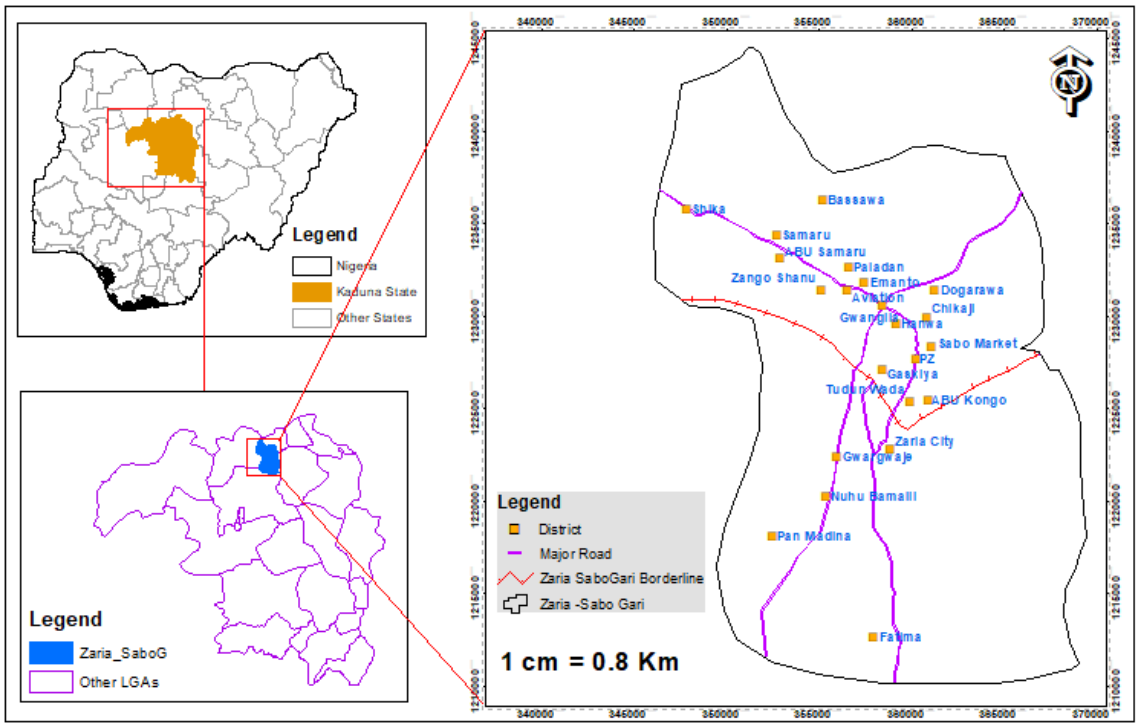

Figure 1 Study Area

3. DATASET AND METHODOLOGY

3.1 Dataset

To execute this study, multi-source geospatial data layer was downloaded and integrated to generate flood triggering and causal factors. Among these multi-source geospatial data, commonly used Shuttle Radar Topographic Mission (SRTM) Digital Elevation Model (DEM) (see for example (Das, 2020a; Elkhrachy, 2015; Hong et al., 2018) and other references herein) was downloaded from USGS website. Another important parameter used in this study for flood mapping is Land Use and Land cover (LULC) (Souissi et al., 2020). Also, as used by the study (Tehrany et al., 2019) is the soil type obtained from International Soil Reference and Information Centre (ISRIC) and Rainfall data (Tehrany et al., 2019) from Tropical Applications of Meteorology Using Satellite Data and Ground-Based Observations (TAMSAT) (Tarnavsky et al., 2014; Maidment et al., 2014, 2017). Summary and other information of the data used are presented in Table 1. The impact of each of the parameters used is presented by (Tehrany et al.,

2019).

Table 1 Data Sources for Flood Vulnerability Mapping

Data	Source	Date	Resolution	Purpose
Landsat OLI/TIRS	United States Geological Survey (USGS) https//earthexplorer.usgs.gov/	15/10/2020	30m	Land use/cover classification
Digital Elevation Model	Shuttle Radar Topographic mission (SRTM) https//earthexplorer.usgs.gov/		1 arc second (approx. 30m)	To visualize the elevation and extract the slope and drainage density, TWI of the study area, which were further processed as factors for flood vulnerability mapping
Rainfall data	Tamsat rainfall estimate version 3.1 https://tamsat.org.uk/	2018	0.0375° (approx. 4km)	To estimate the total annual rainfall within the study area and for subsequent use as a factor in the flood vulnerability analysis
Soil type	International Soil Reference and Information Centre (ISRIC) – World Soil Information https://soilgrids.org/	2020	250m	Processed as a factor for flood vulnerability mapping
Road Network	https://www.openstreetmap.org	2020	-	Distance to road network

3.2 Methodology

To ensure uniformity, all raster data were resampled to 30m. The SRTM DEM for example was utilized to generate the slope map, elevation, and TWI raster datasets. ArcGIS 10.6 was used to process the DEM. In ArcGIS 10.6 software, we used supervised classification with the Maximum Likelihood algorithm to create a land-use land-cover map. Since a total of eight factors were used, AHP was used to define the weights of each factors. Terrset GIS software was used to standardize and generate the weight of each factor used. This was then followed by modelling flood susceptibility using the weighted sum of factors - executed with raster calculator of ArcGIS 10.6 environment. A summary of the step-by-step procedure is presented in Figure 2.

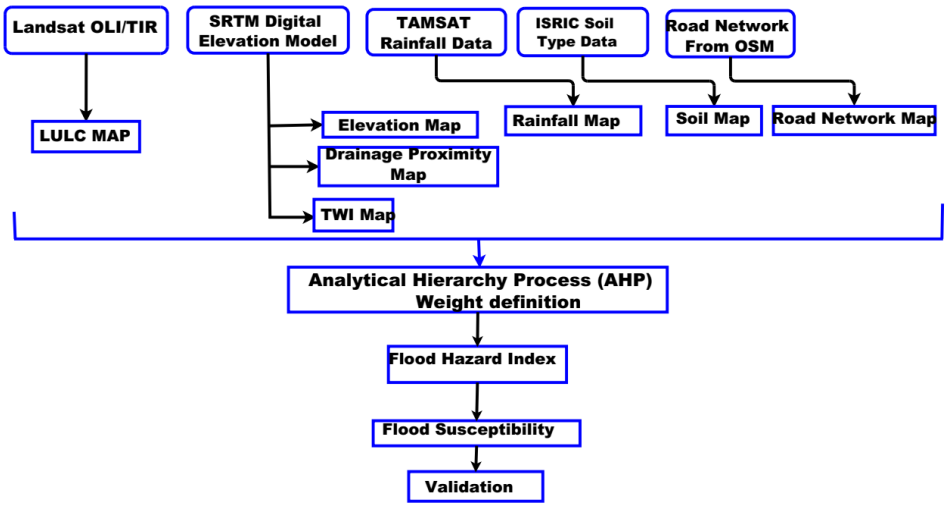

Figure 2 Flow Diagram for the Adopted Methodology

3.3 Analytical Hierarchy Process (AHP)

The AHP, created by (Saaty, 1980), is a model for resolving diverse types of multi-criteria decision problems based on relative precedence assigned to each criterion (Das, 2020b). The benefit of AHP is that it reconciles disparities in a fractional ratio and a existence of large number of software that makes computation more effective and easier

(Calantone et al., 1999; Das, 2020b). According to Das and Gupta, (2021) AHP has the specific goal of preparing a judgmental decision by developing priorities for the selected criteria, with decomposition, relative judgment, and unification of priorities as its main principal components.

Firstly, executing AHP, since the data used for the study are in different format and resolution, Fuzzy method was used for standardization. In the standardization lowest and highest values are in the range of 0 and 1 for all the selected factor. We then choose the multi-criterion parameters. This is then followed by creation of hierarchical structures of selected parameters. We then give subjective values to calculate relative significance and finally aggregate ratings to determine priorities. Table 2 shows the shows the pairwise comparison matrix of flood susceptibility indices. This is an 8 x 8 matrix, with diagonal elements equal one. Consistency ratio (CR) is the computed using Equation 1.

$$\left.\begin{aligned} CR &= \frac{CI}{RI} \\ where\ CI &= \frac{\lambda_{\max} - n}{n-1} \end{aligned}\right\} \qquad (1)$$

Consistency index (CI) is calculated by averaging the value of the consistency vector. RI denotes random index, λ_{max} is the principal eigenvalue of the matrix and n is number of parameters. According to Saaty, (1980) the CR should be less than 0.10. Values greater than 0.10 call for readjustment and re-computation. The value of the consistency ratio for this study is 0.09, which is acceptable.

Table 2 AHP Pair Wise Comparison Matric for Eight Factors

	EL	**LULC**	**R**	**S**	**DP**	**RP**	**TWI**	**ST**	**Computed weight**
EL	1								0.0950
LULC	2	1							0.1023
R	1	3	1						0.2845
S	1	1/3	1/5	1					0.0572
DP	2	3	1/3	7	1				0.1785
RP	1/3	1/5	1/7	1/3	1/5	1			0.0257
TWI	3	2	1/3	5	2	5	1		0.1959
ST	1/2	1	1/4	1/2	1/3	4	1/3	1	0.0608

Elevation (EL), Land Use Land Cover (LULC), Rainfall (R), Drainage proximity (DP), Road proximity (RP), Topographic Wetness Index (TWI), Soil Type (ST)

3.4 Flood Susceptibility Index (FSI)

By using the weighted arithmetic approach of each component with the raster re-classifier tool and Equation 2, the weighed data sets were integrated in the ArcGIS software to create the flood susceptibility map (Elkhrachy, 2015).

$$FSI = \sum_{i=1}^{n} W_i^f * X_i^f \qquad (2)$$

Where FSI denote Flood susceptibility, W_i^f - weight for each factor, X_i^f - Rank of individual factor.

3.5 FSI Validation

Assessment of the precision of the output of a model is crucial, this helps to ascertain the goodness of the model. A prominent method for assessing the accuracy of flood susceptibility map is area under curve (AUC). It has found popularity in numerous studies and considered one of the optimal method in AHP based flood susceptibility models validation (Das, 2020b; Msabi & Makonyo, 2021; Nsangou et al., 2022). For this study, we first divide the Final FSI into 100 classes, the number of pixel for each class was determined. Thereafter, 200 historic locations of flood events obtained from the field with a handheld GPS were overlaid on the resulting map and the number of flood events were determined for each class. The area of each class was equally determined. The AUC was computed based on cumulative rate of the area of each class and flood points sorted from highest to lowest are computed. The false positive rate (FPR) (area of each class) and true positive rate (TPR) (number of flood events in each class) are computed using (ZACH, 2021).

$$FPR = 1 - \frac{FP}{TFP} \qquad (3)$$

$$TPR = 1 - \frac{TP}{TTP} \quad (4)$$

Where FP is the false positive cases, TP is the true positive cases, TTP is the is the total number of true positive cases and TFP is the total number of false positive cases. The AUC of each of each class is thus obtained using

$$AUC = \frac{M}{N} \quad (5)$$

where M is the successive difference of FPR and N is the corresponding TPR.

4. RESULTS AND DISCUSSIONS

4.1 Results

Elevation is among the most triggering factor that contribute to flooding (Das & Gupta, 2021; Hammami et al., 2019; Msabi & Makonyo, 2021)**.** Naturally, water flows from highland (places with higher elevation) to low land area (places with lower elevation) due to the influence of gravity – this causes inundation (Das, 2020a). For the study area, the lowest elevations are around the riverine areas ranging from 693 - 578 meters (Figure 3A). These regions get voluminous discharge and subsequently get flooded faster (Das & Gupta, 2021).

Drainage network is the ratio of the length of all drainage channels within the basin/watershed (in km) to the area of the basin/watershed(in km^2) itself (Elkhrachy, 2015; Ouma & Tateishi, 2014). High drainage network is an indication of high of high surface runoff and vice-versa (Msabi & Makonyo, 2021). The drainage network map generated from SRTM-DEM is presented in Figure 3B.

LULC is a critical parameter in the identification of areas susceptible to flood. Flood can be greatly influenced by the type of land use and land cover in an area. For example, bare land and impervious surfaces are highly susceptible to flooding because of increased surface run-off, while areas with dense vegetation are most likely not prone to flooding (Das & Gupta, 2021; Msabi & Makonyo, 2021). Figure 3C presents the LULC map of the study area. A supervised classification scheme in ArGIS 10.6 was conducted to generate five LULC classes: (i) Bare land (ii) Built-areas (iii) Farmland (iv)Vegetation (v) water bodies.

Studies have shown that heavy downpour (Rainfall) is one of the major causes of flooding. This type of flooding is termed Fluvial flood (Ouma & Tateishi, 2014). When water level in a river, lake, or stream rises and overflows onto its banks, and adjacent land, a fluvial flood occurs (Flood Water, 2020). In the study area, excessive downpour is the major trigger of water level rise. Two dams that supply water to the communities within the study area mostly overflow virtually every year. This exceed the carrying capacity of river channels and hence result to flooding. Figure 3D is spatial pattern of rainfall in the study area.

The importance of the road network cannot be overstated because it connects various locations. Humans prefer to build settlements near roads because of accessibility and proximity. However, during large floods, roads become submerged, causing major communication and accessibility issues. As a result, areas with a high density of roads are more vulnerable (Das, 2020b). The road network obtained from Open Street Map (OSM) (see Table 1) is presented in Figure 3E.

Land surface slope is another important element that contribute to flooding (Elkhrachy, 2015). As the surface slope of an area increases, the more susceptible it is to flooding and vice-versa. It is worth emphasizing that elevation is correlated to slope. Therefore, overland flow, infiltration, and subsurface flow are controlled by the slope. Lithology and soil type are major contributors to slope-related flooding. Rough surfaces associated to soil type and lithology generally slow down flood response, whereas smooth/flat surface quickly respond to flood (Ouma & Tateishi, 2014). Figure 3F presents the percentage slope of the study area. This was generated from the SRTM-DEM (see Table 1). The highest and lowest percentage slope are 86 and 0.5 respectively.

Soil type and structure affect water infiltration process (Das & Gupta, 2021). Silt and clay soil types with fine texture are susceptible to high runoff and poor infiltration and vice versa for the sandy soil with coarse texture. The soil type from ISRIC was used (see Figure 2G). Each of these soil type has properties related or different from the common soil types (sandy, loamy or clayey). Durisols for example (Figure 2G) are relatively deep, free-draining semi-arid regions soils with secondary silica being the coat at the uppermost layer (Staunton et al., 2008). This type of soil is found around river banks and channels (Figure 2G).

TWI is expressed by Equation 6 (Das & Gupta, 2021; Hammami et al., 2019). It is a factor extracted from SRTM-DEM. Where A is the catchment area (m^2) and α (radian) is the slope angle. The higher the value of TWI the more likely the risk of flooding (Das & Gupta, 2021). Figure 5H depicts the distribution of TWI in the study area. Higher

values a more prominent along river channels.

$$TWI = \boldsymbol{ln}\left(\frac{A}{\tan\alpha}\right) \quad (6)$$

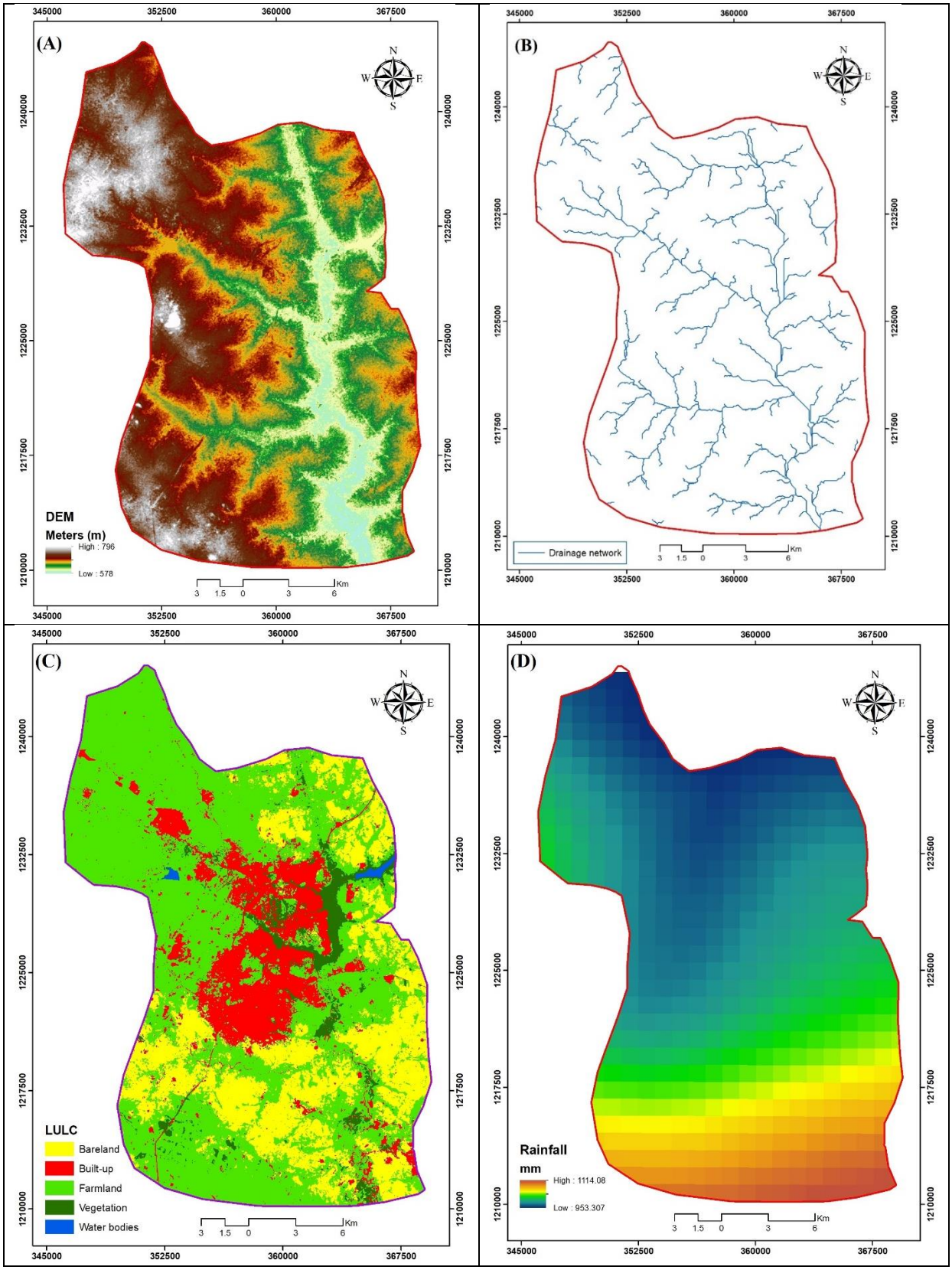

Figure 3 Flood conditioning factors. (A) Altitude, (B) Drainage network, (C) land use land cover (LULC), (D) Rainfall

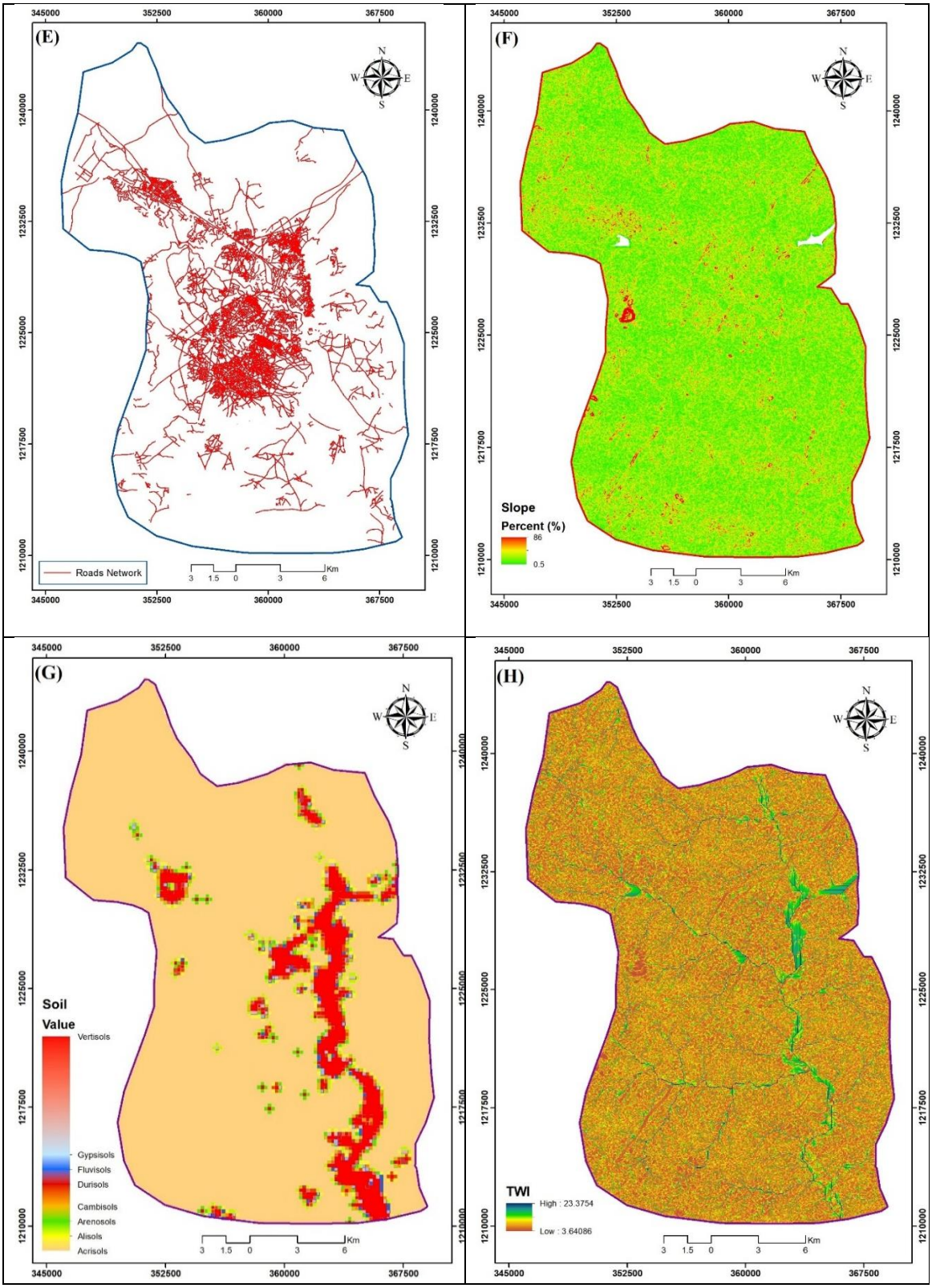

Figure 3 Continued (E) distance from roads network, (F) Slope Map, (G) Soil Map (H) topographic wetness index (TWI)

4.2 Flood Susceptibility Map

The fundamental aim of flood susceptibility mapping is to identify zones of high to low susceptibility. A total of eight multi-source factors, were integrated to generate a flood susceptibility map of urban Zaria. This was done through the modification of equation 2, which is based on weighted linear combination (WLC). In WLC, low score in one component is compensated by high score in another component and vice-versa (Gigović et al., 2017).

$$FSM = EL*0.095 + LULC*0.1023 + R*02845 + S*0.0572 + DP*0.1785 + RP*0.0257 + TWI*0.1959 + ST*0.0608 \quad (7)$$

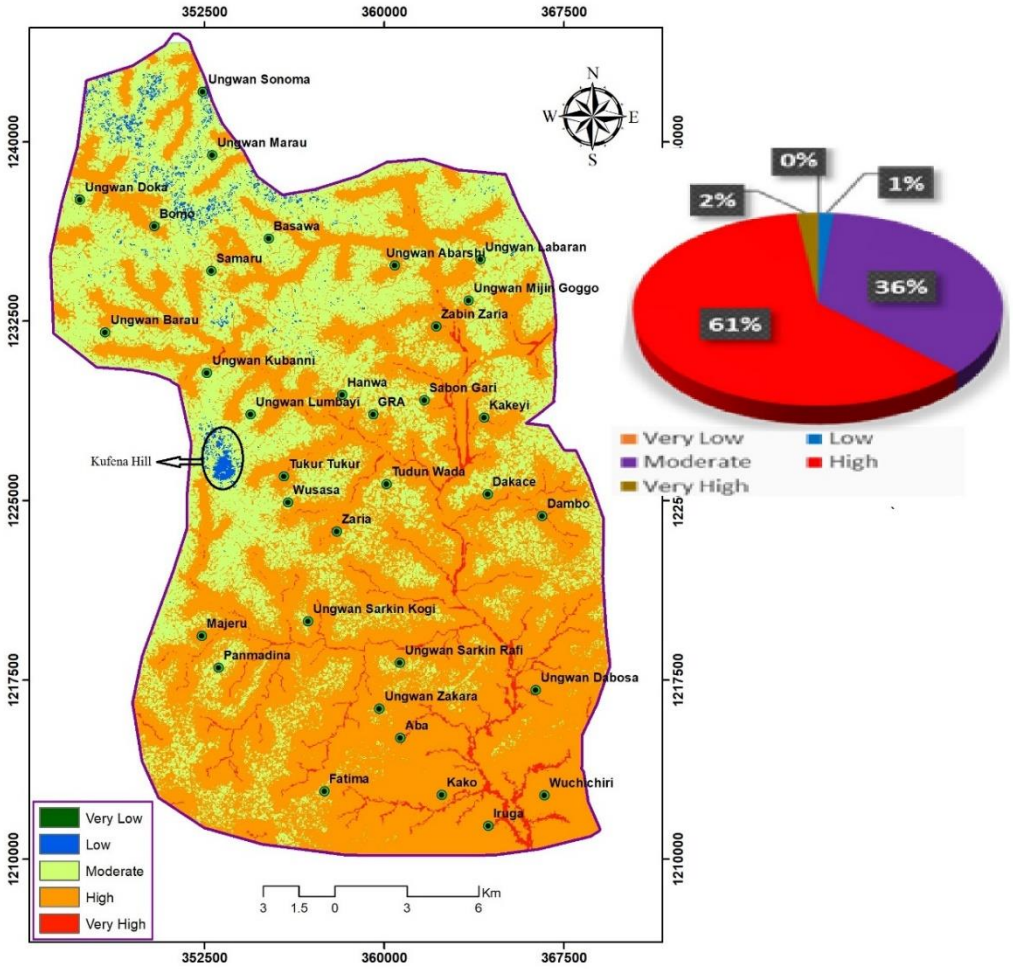

Figure 4 AHP-Based Flood Susceptibility Map of Urban Zaria. Percentage of Area Under Each Class is Presented in the Pie Chat.

The final flood susceptibility map was classified into five (very high, high, moderate, low and very low) different flood susceptible classes. Figure 4 depicts the final flood susceptibility map. From the results, it appears that 61% of the largest area is of the high class, followed by moderate class (36%), very high class 2%, low 1% and very low less than 1%. It is obvious that the most susceptible regions are those around the riverine areas. Communities at the risk of flooding are also indicated in Figure 4.

4.3 Validation

Validation of the precision of the output of any model is crucial. Therefore, assessment of the model is paramount. Popular method is by the use of Area Under Curve (AUC)(Ahmadlou et al., n.d.; Das, 2020b; Das & Gupta, 2021; Msabi & Makonyo, 2021). The AUC computed for this study is 0.860 or 86% accuracy value (Figure 5). AUC value of 1 is considered very accurate and without bias while more than 0.8 is considered accurate and acceptable(Das, 2020b). Therefore, this indicates the accuracy of the proposed FSI.

4.4 Discussion

Figure 4 indicates that very high susceptible regions are regions around river bank and channels. By implication, settlements around these regions are extremely prone to flood events. A watch out are Iruga, Kako, Wuchichiri, Ungwan Dabosa, amongst others. A worrying scenario is shown in Figure 6 (for example around Tudun wada) where people build houses and farm around river channels during both dry and raining season. This calls for necessary action by the authorities concerned, so as to avert loss of lives and property. Among these action is to build irrigation canals. The high susceptible regions are those around flat or low elevations. The low susceptible regions are rocky and hilly (e.g Kufena hill) with very high elevation. Interestingly, North Eastern region of Urban Zaria e.g. Bomo, Samaru Basawa, Ungwna Marau are moderately to low susceptible to flood. Finally, rainfall, followed by TWI,

LULC and drainage proximity are respectively the main parameters responsible for flooding.

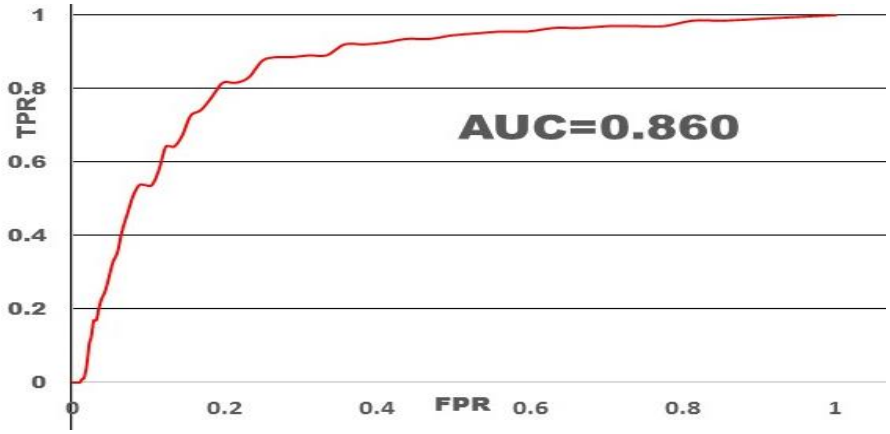

Figure 5 Area Under the Uurve (AUC) related to FSI model.

Figure 6 Activities Along Tudun/Wada watershed

5 CONCLUSIONS

For future flood events, flood susceptibility mapping should be given so much emphasis so as to avert the negative effect of the aftermath. This study therefore proposes a methodology for delineating flood susceptible areas in urban Zaria. By considering eight factors from multi-source geospatial data and geographic information system, AHP multi criteria decision analysis (MCDA) method was used. The outcome of the study based on five classes revealed a large area that fall under high (61%) and moderate (36%). Very high accounted for about 2% of the study area. Finally, low and very low accounted for about 1% and less than one 1% respectively. A metric for assessing the accuracy of FSI is the AUC. An AUC of 0.86 revealed the goodness of the developed FSI for urban Zaria.

REFERENCES

Ahmadlou, M., Al-Fugara, A., Al-Shabeeb, A. R., Arora, A., Al-Adamat, R., Pham, Q. B., Al-Ansari, N., Linh, N. T. T., & Sajedi, H. n.d.. Flood susceptibility mapping and assessment using a novel deep learning model combining multilayer perceptron and autoencoder neural networks. *Journal of Flood Risk Management*, *n/a*(n/a), e12683. https://doi.org/10.1111/jfr3.12683

Andongma, W. T., Kudamnya, E. A., & Gajere, J. N. 2017. Flood Risk Assesment of Zaria Metropolis and Environs: A GIS Approach. *Asian Journal of Environment & Ecology*, 1–8. https://doi.org/10.9734/AJEE/2017/32456

Beck, H. E., Zimmermann, N. E., McVicar, T. R., Vergopolan, N., Berg, A., & Wood, E. F. 2018. Present and future

Köppen-Geiger climate classification maps at 1-km resolution. *Scientific Data*, *5*(1), 1–12. https://doi.org/10.1038/sdata.2018.214
Cabrera, J. S., & Lee, H. S. 2019. Flood-Prone Area Assessment Using GIS-Based Multi-Criteria Analysis: A Case Study in Davao Oriental, Philippines. *Water*, *11*(11), 2203. https://doi.org/10.3390/w11112203
Calantone, R. J., Di Benedetto, C. A., & Schmidt, J. B. (1999). Using the Analytic Hierarchy Process in New Product Screening. *Journal of Product Innovation Management*, *16*(1), 65–76. https://doi.org/10.1111/1540-5885.1610065
Caruso, G. D. 2017. The legacy of natural disasters: The intergenerational impact of 100 years of disasters in Latin America. *Journal of Development Economics*, *127*, 209–233. https://doi.org/10.1016/j.jdeveco.2017.03.007
Dano, U. L., Balogun, A.-L., Matori, A.-N., Wan Yusouf, K., Abubakar, I. R., Said Mohamed, M. A., Aina, Y. A., & Pradhan, B. 2019. Flood Susceptibility Mapping Using GIS-Based Analytic Network Process: A Case Study of Perlis, Malaysia. *Water*, *11*(3), 615. https://doi.org/10.3390/w11030615
Das, S. 2020a. Flood susceptibility mapping of the Western Ghat coastal belt using multi-source geospatial data and analytical hierarchy process (AHP). *Remote Sensing Applications: Society and Environment*, *20*, 100379. https://doi.org/10.1016/j.rsase.2020.100379
Das, S. 2020b. Flood susceptibility mapping of the Western Ghat coastal belt using multi-source geospatial data and analytical hierarchy process (AHP). *Remote Sensing Applications: Society and Environment*, *20*, 100379. https://doi.org/10.1016/j.rsase.2020.100379
Das, S., & Gupta, A. 2021. Multi-criteria decision based geospatial mapping of flood susceptibility and temporal hydro-geomorphic changes in the Subarnarekha basin, India. *Geoscience Frontiers*, *12*(5), 101206. https://doi.org/10.1016/j.gsf.2021.101206
Dennis, P. W. C. 1944. The district around Zaria, Northern Nigeria. *Scottish Geographical Magazine*, *60*(1), 15–19. https://doi.org/10.1080/00369228708735257
Elkhrachy, I. 2015. Flash Flood Hazard Mapping Using Satellite Images and GIS Tools: A case study of Najran City, Kingdom of Saudi Arabia (KSA). *The Egyptian Journal of Remote Sensing and Space Science*, *18*(2), 261–278. https://doi.org/10.1016/j.ejrs.2015.06.007
Flood Water. 2020, July 22. *Three common types of flood explained*. Three Common Types of Flood Explained. https://www.zurich.com/en/knowledge/topics/flood-and-water-damage/three-common-types-of-flood
floodlist. 2021, February 12. *FloodList*. http://floodlist.com/
Gigović, L., Pamučar, D., Bajić, Z., & Drobnjak, S. 2017. Application of GIS-Interval Rough AHP Methodology for Flood Hazard Mapping in Urban Areas. *Water*, *9*(6), 360. https://doi.org/10.3390/w9060360
Hammami, S., Zouhri, L., Souissi, D., Souei, A., Zghibi, A., Marzougui, A., & Dlala, M. 2019. Application of the GIS based multi-criteria decision analysis and analytical hierarchy process (AHP) in the flood susceptibility mapping (Tunisia). *Arabian Journal of Geosciences*, *12*(21), 653. https://doi.org/10.1007/s12517-019-4754-9
Hong, H., Panahi, M., Shirzadi, A., Ma, T., Liu, J., Zhu, A.-X., Chen, W., Kougias, I., & Kazakis, N. 2018. Flood susceptibility assessment in Hengfeng area coupling adaptive neuro-fuzzy inference system with genetic algorithm and differential evolution. *Science of The Total Environment*, *621*, 1124–1141. https://doi.org/10.1016/j.scitotenv.2017.10.114
Huang, Y., & Qin, X. 2014. Uncertainty analysis for flood inundation modelling with a random floodplain roughness field. *Environmental Systems Research*, *3*(1), 9. https://doi.org/10.1186/2193-2697-3-9
Maidment, R. I., Grimes, D., Allan, R. P., Tarnavsky, E., Stringer, M., Hewison, T., Roebeling, R., & Black, E. 2014. The 30 year TAMSAT African Rainfall Climatology And Time series (TARCAT) data set. *Journal of Geophysical Research: Atmospheres*, *119*(18), 10,619-10,644. https://doi.org/10.1002/2014JD021927
Maidment, R. I., Grimes, D., Black, E., Tarnavsky, E., Young, M., Greatrex, H., Allan, R. P., Stein, T., Nkonde, E., Senkunda, S., & Alcántara, E. M. U. 2017. A new, long-term daily satellite-based rainfall dataset for operational monitoring in Africa. *Scientific Data*, *4*(1), 170063. https://doi.org/10.1038/sdata.2017.63
Mangaji, S. R., Mukhtar, I., Iguisi, E. O., Isma'il, M., & Salisu, A. 2020. Analysis of Flood Vulnerability in Unplanned Settlements along the Bank of River Kubanni, Zaria, Nigeria. *African Scholar Journal of Environmental Design & Construction Managt*, *18*(4). https://www.africanscholarpublications.com/african-scholar-journal-of-environmental-design-construction-managt-vol-18-no-4/
Msabi, M. M., & Makonyo, M. 2021. Flood susceptibility mapping using GIS and multi-criteria decision analysis: A case of Dodoma region, central Tanzania. *Remote Sensing Applications: Society and Environment*, *21*, 100445. https://doi.org/10.1016/j.rsase.2020.100445
Nsangou, D., Kpoumié, A., Mfonka, Z., Ngouh, A. N., Fossi, D. H., Jourdan, C., Mbele, H. Z., Mouncherou, O. F., Vandervaere, J.-P., & Ndam Ngoupayou, J. R. 2022. Urban flood susceptibility modelling using AHP and GIS approach: Case of the Mfoundi watershed at Yaoundé in the South-Cameroon plateau. *Scientific African*, *15*, e01043. https://doi.org/10.1016/j.sciaf.2021.e01043
Ouma, Y. O., & Tateishi, R. 2014. Urban Flood Vulnerability and Risk Mapping Using Integrated Multi-Parametric AHP and GIS: Methodological Overview and Case Study Assessment. *Water*, *6*(6), 1515–1545. https://doi.org/10.3390/w6061515
Razavi Termeh, S. V., Pourghasemi, H. R., & Alidadganfard, F. 2018. Flood Inundation Susceptibility Mapping using Analytical Hierarchy Process (AHP) and TOPSIS Decision Making Methods and Weight of Evidence Statistical

Model (Case Study: Jahrom Township, Fars Province). *Journal of Watershed Management Research*, *9*(17), 67–81. https://doi.org/10.29252/jwmr.9.17.67
Rentschler, J., & Salhab, M. 2020. *People in Harm's Way: Flood Exposure and Poverty in 189 Countries*. The World Bank. https://doi.org/10.1596/1813-9450-9447
Rincón, D., Khan, U. T., & Armenakis, C. 2018. Flood Risk Mapping Using GIS and Multi-Criteria Analysis: A Greater Toronto Area Case Study. *Geosciences*, *8*(8), 275. https://doi.org/10.3390/geosciences8080275
Saaty, T. L. 1980. *The Analytic Hierarchy Process: Planning, Priority Setting, Resource Allocation*. McGraw-Hill.
Souissi, D., Zouhri, L., Hammami, S., Msaddek, M. H., Zghibi, A., & Dlala, M. (2020). GIS-based MCDM – AHP modeling for flood susceptibility mapping of arid areas, southeastern Tunisia. *Geocarto International*, *35*(9), 991–1017. https://doi.org/10.1080/10106049.2019.1566405
Staunton, S., Fairbridge, R. W., & Spaargaren, O. 2008. Durisols. In W. Chesworth (Ed.), *Encyclopedia of Soil Science* (pp. 198–199). Springer Netherlands. https://doi.org/10.1007/978-1-4020-3995-9_169
Tarnavsky, E., Grimes, D., Maidment, R., Black, E., Allan, R. P., Stringer, M., Chadwick, R., & Kayitakire, F. (2014). Extension of the TAMSAT Satellite-Based Rainfall Monitoring over Africa and from 1983 to Present. *Journal of Applied Meteorology and Climatology*, *53*(12), 2805–2822. https://doi.org/10.1175/JAMC-D-14-0016.1
Tehrany, M. S., Kumar, L., & Shabani, F. 2019. A novel GIS-based ensemble technique for flood susceptibility mapping using evidential belief function and support vector machine: Brisbane, Australia. *PeerJ*, *7*, e7653. https://doi.org/10.7717/peerj.7653
Tehrany, M. S., Pradhan, B., & Jebur, M. N. 2013. Spatial prediction of flood susceptible areas using rule based decision tree (DT) and a novel ensemble bivariate and multivariate statistical models in GIS. *Journal of Hydrology*, *504*, 69–79. https://doi.org/10.1016/j.jhydrol.2013.09.034
Veleda, S., Martínez-Graña, A., Santos-Francés, F., Sánchez-SanRoman, J., & Criado, M. 2017. Analysis of the Hazard, Vulnerability, and Exposure to the Risk of Flooding (Alba de Yeltes, Salamanca, Spain). *Applied Sciences*, *7*(2), 157. https://doi.org/10.3390/app7020157
Yalcin, G., & Akyürek, Z. 2004. Analysing flood vulnerable area with multicriteria evaluation. *Proceedings of the 20th ISPRS Congress*, 359–364.
ZACH. 2021. August 9. How to Create a ROC Curve in Excel (Step-by-Step). *Statology*. https://www.statology.org/roc-curve-excel/